Influence of Induced Magnetic Field and Partial Slip on the Peristaltic Flow of a Couple Stress Fluid in an Asymmetric Channel

Akram, Safia*[+]

Department of Basic Sciences, MCS, National University of Sciences and Technology, Islamabad, PAKISTAN

Nadeem, S.; Hussain, Anwar

Department of Mathematics, Quaid-i-Azam University 45320, Islamabad 44000, PAKISTAN

ABSTRACT: *This paper describes the effects of induced magnetic field and partial slip on the peristaltic flow of a couple stress fluids in an asymmetric channel. The two dimensional equation of couple stress fluid are simplified by making the assumptions of long wave length and low Reynolds number. The exact solutions of reduced momentum equation and magnetic force function have been computed in wave frame. The expressions for stream function, magnetic force function and pressure rise per wave length have been also computed. Finally, the pressure rise, pressure gradient, velocity, magnetic force function and stream lines for different physical parameters of interest are plotted.*

KEY WORDS: *Induced magnetic field, Couple stress fluid, Partial slip, Peristaltic flow, Asymmetric channel.*

INTRODUCTION

Since, the first investigation done by *Stokes* [1] on the couple stress fluid, a large number of studies containing couple stress model with different geometries have been discussed by many researchers [2-9]. This model is the simplest generalization of classical Navier-Stokes model, and has distinct features which allows for polar effects in addition to possessing large viscosity, such as pressure of couple stress and body couples.

Peristaltic pumping is a form of fluid transport that occurs when a progressive wave of area contraction or expansion propagates along the length of a distensible tube containing the fluid. Peristaltic flow occurs widely in urine transport from kidney to bladder, swallowing food through the esophagus, movement of chyme in the gastrointestinal tract, transport of spermatozoa in the ducts efferentes of the male reproductive tract, movement of ovum in the female fallopian tubes, vasomotion of small blood vessels, transport of slurries, corrosive fluids, sanitary fluids and noxious fluids in nuclear industry. In view, of these applications, number of studies has been made which involve Newtonian and Non-Newtonian fluids with different kind of geometries [10-22].

The effects of MHD on the peristaltic flow problems have applications in physiological fluids such as blood

***** *To whom correspondence should be addressed.*

+ E-mail: drasafiaakram@gmail.com ; safia_akram@yahoomail.com

1021-9986/14/3/ 10/$/3.10

flow, blood pump machines and with the need for theoretical research on the operation of peristaltic MHD compressor. Further, the application of magnetic field occurs in the form of a device MRI (Magnetic Resonance Imaging), which is used for diagnosis of brain, vascular diseases and all the human body. *Mekheimer* [23] has discussed the effects of the induced magnetic field on the peristaltic flow of a couple stress fluid in a slit channel. *Srivastava & Agrawal* [24] discussed the effects of MHD on blood flow.

In the studies mentioned above, no slip conditions have been used. There are very few attempts in which non-standards boundary conditions are used. Mention may be made to the interesting works of [25-28]. However, no attempt has been made to study the effect of partial slip on the peristaltic flow of a couple stress fluid in an asymmetric channel. The interest of this paper is to present unified solution for the different facets of the problem arising in Non-Newtonian fluids. These include peristaltic problems in couple stress fluid, partial slip boundary conditions and the applications of induced magnetic field. An exact solution of momentum and magnetic induction equation has been found. The boundary condition for partial slip needs to be modified for couple stress fluid because of the appropriate choice of the shear stress in couple stress fluid. The graphical results are also presented to gauge the effects of certain physical parameters. Finally, the trapping phenomena for different physical parameters have also been discussed pictorically.

THEORITICAL SECTION

Mathematical model and the governing equations

Let us consider the peristaltic flow of an incompressible, electrically conducting couple stress fluid in a two dimensional channel of width $d_1' + d_2'$. The flow is generated by sinusoidal wave trains propagating with constant speed c along the channel walls. We choose rectangular coordinate system for the channel with X' along the centerline of the channel and Y' is transverse to it. An external transverse uniform constant magnetic field H'_0, induced magnetic field $H'(h'_{X'}(X',Y',t'), H'_0 + h'_{Y'}(X',Y',t'), 0)$ and the total magnetic field $H'^{+}(h'_{X'}(X',Y',t'), H_0 + h'_{Y}(X',Y',t'$ are taken into account. Finally, the channel walls are considered to be non-conductive and the geometry of the wall surface is defined as

$$h'_1(X',t') = d_1' + a_1' \cos[\frac{2\pi}{\lambda}(X' - ct')], \tag{1}$$

$$h_2'(X',t') = -d_2' - b_1' \cos[\frac{2\pi}{\lambda}(X' - ct') + \varphi],$$

where a_1' and b_1' are the amplitudes of the waves, λ is the wave length, $d_1' + d_2'$ is the width of the channel, c is the velocity of propagation, t' is the time and X' is the direction of wave propagation. The phase difference ϕ varies in the range $0 \le \varphi \le \pi$ in which $\varphi = 0$ corresponds to symmetric channel with waves out of phase and $\varphi = \pi$, the waves are in phase, further, a_1', b_1', d_1', d_2' and ϕ satisfies the condition

$$a_1'^2 + b_1'^2 + 2a_1'b_1' \cos\varphi \le \left(d_1' + d_2'\right)^2.$$

The non-dimensional equations which govern the MHD flow for a couple stress fluid in the wave frame are directly written as [23].

$$\frac{\partial u}{\partial x} + \frac{\partial v}{\partial y} = 0, \tag{2}$$

$$\mathrm{Re}\,\delta(u\frac{\partial}{\partial x} + v\frac{\partial}{\partial y})u = -\frac{\partial p_m}{\partial x} + \nabla^2 u - \frac{1}{\gamma^2}\nabla^4 u + \tag{3}$$

$$\mathrm{Re}\,S^2\frac{\partial(hx)}{\partial y} + \mathrm{Re}\,S^2\delta(h_x\frac{\partial}{\partial x} + h_y\frac{\partial}{\partial y})h_x,$$

$$u\frac{\partial}{\partial x} + v\frac{\partial}{\partial y})v = -\frac{\partial p_m}{\partial y} + \delta^2\nabla^2 v - \frac{\delta^2}{\gamma^2}\nabla^2 v + \tag{4}$$

$$\mathrm{Re}\,S^2\delta^2\frac{\partial(hy)}{\partial y} + \mathrm{Re}\,S^2\delta^3(h_x\frac{\partial}{\partial x} + h_y\frac{\partial}{\partial y})h_y,$$

$$u + \delta(uh_y - vh_x) + \frac{1}{R_m}(\frac{\partial(h_x)}{\partial y} - \delta^2\frac{\partial(h_y)}{\partial x}) = E, \tag{5}$$

where

$$x' = X' - ct', \quad y' = Y', u' = U' - c, \quad v' = V',$$

$$x = \frac{x'}{\lambda},\ y = \frac{y'}{d_1'},\ u = \frac{u'}{c},\ v = \frac{v'}{c\delta},\ h = \frac{h'(x')}{d_1'},$$

$$p = \frac{d_1'^2}{\lambda\mu c}p'(x'),\ t = \frac{ct'}{\lambda},\ \psi = \frac{\psi'}{cd_1'},\ \Phi = \frac{\Phi'}{H_0 d_1'},\ u = \frac{\partial\psi}{\partial y},$$

$$v = -\frac{\partial\psi}{\partial x},\ h_x = \frac{\partial\Phi}{\partial y},\ h_y = -\delta\frac{\partial\Phi}{\partial x},\ \mathrm{Re} = \frac{cd_1'\rho}{\mu},$$

$$\delta = \frac{d_1'}{\lambda},\ S = \frac{H_0}{c}\sqrt{\frac{\mu_e}{\rho}},\ R_m = \sigma\mu_e ac,\ \gamma = \sqrt{\frac{\mu}{\eta}}d_1',$$

$$a = \frac{a_1'}{d_1'},\ \ b = \frac{b_1'}{d_1'}\ \ \nabla^2 = \delta^2\frac{\partial^2}{\partial x^2} + \frac{\partial^2}{\partial y^2}.$$

The corresponding dimensionless boundary conditions are

$$u + \beta\left(\frac{\partial u}{\partial y} - \frac{1}{\gamma^2}\frac{\partial^3 u}{\partial y^3}\right) = -1, \quad v = \frac{dh_1}{dx}, \tag{6}$$

$$-(\delta^4\frac{\partial^2 v}{\partial x^2} - \delta^2\frac{\partial^2 u}{\partial x\partial y})\frac{dh_1}{dx} + \delta^2\frac{\partial^2 v}{\partial x\partial y} - \frac{\partial^2 u}{\partial y^2} = 0 \quad \text{at } y = h_1.$$

$$u - \beta\left(\frac{\partial u}{\partial y} - \frac{1}{\gamma^2}\frac{\partial^3 u}{\partial y^3}\right) = -1, \quad v = \frac{dh_2}{dx}, \tag{7}$$

$$-(\delta^4\frac{\partial^2 v}{\partial x^2} - \delta^2\frac{\partial^2 u}{\partial x\partial y})\frac{dh_2}{dx} + \delta^2\frac{\partial^2 v}{\partial x\partial y} - \frac{\partial^2 u}{\partial y^2} = 0 \quad \text{at } y = h_2.$$

In which β represent the slip length (β=0 correspond to no slip).

Using the assumption of long wave length and low Reynolds number, Eqs. (2) to (7) reduces to

$$\frac{\partial p}{\partial x} = \frac{\partial^2 u}{\partial y^2} - \frac{1}{\gamma^2}\frac{\partial^4 u}{\partial y^4} + ReS^2\frac{\partial(h_x)}{\partial y}, \tag{8}$$

$$\frac{\partial p}{\partial y} = 0, \tag{9}$$

$$u + \frac{1}{R_m}\frac{\partial(h_x)}{\partial y} = E, \tag{10}$$

$$u + \beta\left(\frac{\partial u}{\partial y} - \frac{1}{\gamma^2}\frac{\partial^3 u}{\partial y^3}\right) = -1, \quad v = \frac{dh_1}{dx}, \quad \frac{\partial^2 u}{\partial y^2} = 0 \ \text{ at} \tag{11}$$

$$y = h_1 = 1 + a\cos 2\pi x,$$

$$u - \beta\left(\frac{\partial u}{\partial y} - \frac{1}{\gamma^2}\frac{\partial^3 u}{\partial y^3}\right) = -1, \quad v = \frac{dh_2}{dx}, \quad \frac{\partial^2 u}{\partial y^2} = 0 \ \text{ at} \tag{12}$$

$$y = h_2 = -d - b\cos(2\pi x + \varphi)$$

From Eqs. (8) and (10), we can write

$$\frac{\partial p}{\partial x} = \frac{\partial^2 u}{\partial y^2} - \frac{1}{\gamma^2}\frac{\partial^4 u}{\partial y^4} + ReS^2(E-u)R_m. \tag{13}$$

The dimensionless mean flow θ is defined by [9]

$$\theta = F + 1 + d,$$

where

$$F = \int_{h_1}^{h_2} u\,dy \tag{14}$$

Exact solution

Eq. (13) is linear, non-homogeneous fourth order differential equation whose exact solution can be written as

$$u = A\cosh(m_1 y) + B\sinh(m_1 y) + C\cosh(m_2 y) + D\sinh(m_2 y) + E - \frac{1}{M^2}\frac{dp}{dx}, \tag{15}$$

where A to D are constants , $M^2 = ReS^2R_m$ and $m_{1,2} = \frac{\gamma}{\sqrt{2}}\left(1 \pm \sqrt{1 - \frac{4M^2}{\gamma^2}}\right)^{\frac{1}{2}}$.

Invoking the boundary conditions we get

$$A = \frac{-\left(2m_2^2\left((1+E)M^2 - \frac{dp}{dx}\right)\cosh\left[\frac{(h_1+h_2)m_1}{2}\right]\cosh\left[\frac{(h_1-h_2)m_2}{2}\right]\right)}{M^2\left(\left(m_2^2-m_1^2\right)\cosh\left[\frac{(h_1-h_2)(m_1-m_2)}{2}\right] + \left(m_2^2-m_1^2\right)\cosh\left[\frac{(h_1-h_2)(m_1+m_2)}{2}\right]\right) + m_1m_2\beta\left((m_1+m_2)\sinh\left[\frac{(h_1-h_2)(m_1-m_2)}{2}\right] + (m_2-m_1)\sinh\left[\frac{(h_1-h_2)(m_1+m_2)}{2}\right]\right)} \tag{16}$$

$$B = \frac{2m_2^2\left((1+E)M^2 - \frac{dp}{dx}\right)\sinh\left[\frac{(h_1+h_2)m_1}{2}\right]\cosh\left[\frac{(h_1-h_2)m_2}{2}\right]}{M^2\left(\left(m_2^2-m_1^2\right)\cosh\left[\frac{(h_1-h_2)(m_1-m_2)}{2}\right] + \left(m_2^2-m_1^2\right)\cosh\left[\frac{(h_1-h_2)(m_1+m_2)}{2}\right]\right) + m_1m_2\beta\left((m_1+m_2)\sinh\left[\frac{(h_1-h_2)(m_1-m_2)}{2}\right] + (m_2-m_1)\sinh\left[\frac{(h_1-h_2)(m_1+m_2)}{2}\right]\right)}$$

$$C=\frac{2m_1^2\left((1+E)M^2-\frac{dp}{dx}\right)\cosh\left[\frac{(h_1+h_2)m_2}{2}\right]\cosh\left[\frac{(h_1-h_2)m_1}{2}\right]}{M^2\left(\left(m_2^2-m_1^2\right)\cosh\left[\frac{(h_1-h_2)(m_1-m_2)}{2}\right]+\left(m_2^2-m_1^2\right)\cosh\left[\frac{(h_1-h_2)(m_1+m_2)}{2}\right]\right)+ m_1m_2\beta\left((m_1+m_2)\sinh\left[\frac{(h_1-h_2)(m_1-m_2)}{2}\right]+(m_2-m_1)\sinh\left[\frac{(h_1-h_2)(m_1+m_2)}{2}\right]\right)}$$

$$D=\frac{2m_1^2\left((1+E)M^2-\frac{dp}{dx}\right)\sinh\left[\frac{(h_1+h_2)m_2}{2}\right]\cosh\left[\frac{(h_1-h_2)m_1}{2}\right]}{M^2\left(\left(m_1^2-m_2^2\right)\cosh\left[\frac{(h_1-h_2)(m_1-m_2)}{2}\right]+\left(m_1^2-m_2^2\right)\cosh\left[\frac{(h_1-h_2)(m_1+m_2)}{2}\right]\right)+ m_1m_2\beta\left(-(m_1+m_2)\sinh\left[\frac{(h_1-h_2)(m_1-m_2)}{2}\right]+(m_1-m_2)\sinh\left[\frac{(h_1-h_2)(m_1+m_2)}{2}\right]\right)}$$

The corresponding stream function is

$$\psi=\frac{A}{m_1}\sinh(m_1y)+\frac{B}{m_1}\cosh(m_1y)+ \frac{C}{m_2}\sinh(m_2y)+\frac{D}{m_2}\cosh(m_2y)+\left(E-\frac{1}{M^2}\frac{dp}{dx}\right)y, \quad (17)$$

From Eqs.(14) to (17), the expression for pressure gradient is defined as

$$\frac{dp}{dx}=-\frac{M^2}{a_{09}}\left(-a_{01}-a_{02}+a_{03}-a_{04}\right). \quad (18)$$

where

$$a_{01}=\left(F+(h_1-h_2)E\right)m_1\left(m_1^2-m_2^2\right)\times \cosh\left[\frac{(h_1-h_2)(m_1-m_2)}{2}\right], \quad (19)$$

$$a_{02}=\left(F+(h_1-h_2)E\right)m_1\left(m_1^2-m_2^2\right)\times \cosh\left[\frac{(h_1-h_2)(m_1+m_2)}{2}\right],$$

$$a_{03}=\left(-2(1+E)\left(m_1^2+m_2^2\right)+\left(F+(h_1-h_2)E\right)m_1^2m_2(m_1+m_2)\beta\right)\times \sinh\left[\frac{(h_1-h_2)(m_1-m_2)}{2}\right]$$

$$a_{04}=(m_1-m_2)\left(-2(1+E)(m_1+m_2)+\left(F+(h_1-h_2)E\right)m_1^2m_2\beta\right)\times \sinh\left[\frac{(h_1-h_2)(m_1+m_2)}{2}\right],$$

$$a_{05}=(h_1-h_2)m_1\left(m_1^2-m_2^2\right)\cosh\left[\frac{(h_1-h_2)(m_1-m_2)}{2}\right]$$

$$a_{06}=(h_1-h_2)m_1\left(m_1^2-m_2^2\right)\cosh\left[\frac{(h_1-h_2)(m_1+m_2)}{2}\right],$$

$$a_{07}=\left(2m_2^2+m_1^2(2-(h_1-h_2)m_2(m_1+m_2)\beta)\right)\times \sinh\left[\frac{(h_1-h_2)(m_1-m_2)}{2}\right],$$

$$a_{08}=(m_1-m_2)(-2(m_1+m_2)+(h_1-h_2)m_1^2m_2\beta)\times \sinh\left[\frac{(h_1-h_2)(m_1+m_2)}{2}\right],$$

$$a_{09}=a_{05}+a_{06}+a_{07}+a_{08}.$$

Using $h_x=\frac{\partial\Phi}{\partial y}$ in Eq. (10), we get the magnetic force function in the form

$$\frac{\partial^2\Phi}{\partial y^2}=(E-u)R_m, \quad (20)$$

The corresponding boundary conditions are

$\Phi=0$ at $y=h_1$ and $y=h_2$.

The exact solution of Eq. (19) satisfying the boundary condition (20) can be written as

$$\Phi=\frac{R_m}{M^2}\frac{dp}{dx}\frac{y^2}{2}+c_1y+c_2, \quad (21)$$

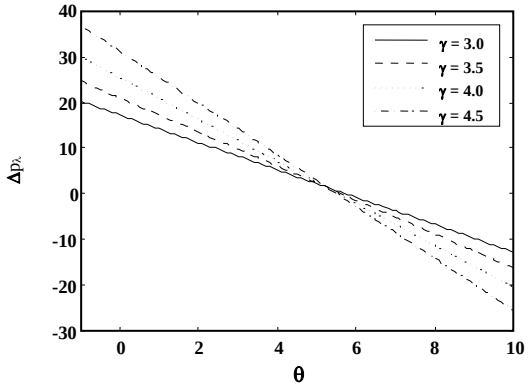

Fig. 1: Variation of Δp_λ with θ for different values of γ at a=0.7, b=1.2, d=2, $\varphi = \frac{\pi}{2}$, M=1, E=6, β=0.02.

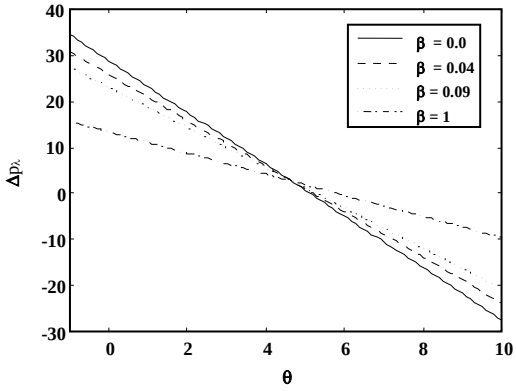

Fig. 2: Variation of Δp_λ with θ for different values of β at a=0.7, b=1.2, d=2, $\varphi = \frac{\pi}{2}$, M=1, E=6, γ=3.5.

$$-R_m\left(\begin{array}{l}\frac{A}{m_1^2}\cosh(m_1y)+\frac{B}{m_1^2}\sinh(m_1y)+\\ \frac{C}{m_2^2}\cosh(m_2y)+\frac{D}{m_2^2}\sinh(m_2y)\end{array}\right)$$

where

$$c_1=\frac{R_m}{2(h_1-h_2)M^2m_1^2m_2^2}\left(\frac{dp}{dx}\left(h_2^2-h_1^2\right)m_1^2m_2^2+b_0\right)$$

$$c_2=\frac{R_m}{2(h_1-h_2)M^2m_1^2m_2^2}\left(\frac{dp}{dx}\left(h_2h_1^2-h_2^2h_1\right)m_1^2m_2^2+b_1\right)$$

$$b_0=\left(\begin{array}{l}2AM^2m_2^2\left(\cosh(h_1m_1)-\cosh(h_2m_1)\right)+\\ 2BM^2m_2^2\left(\sinh(h_1m_1)-\sinh(h_2m_1)\right)\\ \\ +2CM^2m_1^2\left(\cosh(h_1m_2)-\cosh(h_2m_2)\right)+\\ 2DM^2m_1^2\left(\sinh(h_1m_2)-\sinh(h_2m_2)\right)\end{array}\right)$$

$$b_1=\left(\begin{array}{l}2AM^2m_2^2\left(-h_2\cosh(h_1m_1)+h_1\cosh(h_2m_1)\right)+\\ 2BM^2m_2^2\left(-h_2\sinh(h_1m_1)+h_1\sinh(h_2m_1)\right)\\ \\ +2CM^2m_1^2\left(-h_2\cosh(h_1m_2)+h_1\cosh(h_2m_2)\right)+\\ 2DM^2m_1^2\left(-h_2\sinh(h_1m_2)+h_1\sinh(h_2m_2)\right)\end{array}\right)$$

and A to D are defined in Eq. (16).

Now the expression of axial induced magnetic field is calculated from Eq. (21) by using $\left(h_x=\frac{\partial\Phi}{\partial y}\right)$

$$h_x(x,y)=\frac{R_m}{M^2}\frac{dp}{dx}y+c_1-R_m\left(\frac{A}{m_1}\sinh(m_1y)+\right. \quad (22)$$
$$\left.\frac{B}{m_1}\cosh(m_1y)+\frac{C}{m_2}\sinh(m_2y)+\frac{D}{m_2}\cosh(m_2y)\right)$$

Also the current density distribution takes the following form

$$J_z(x,y)=\frac{R_m}{M^2}\frac{dp}{dx}+-R_m\left(A\cosh(m_1y)+\right. \quad (23)$$
$$\left.B\sinh(m_1y)+C\cosh(m_2y)+D\sinh(m_2y)\right)$$

The non-dimensional expression for the pressure rise per wavelength Δp_λ, is defined as

$$\Delta p_\lambda=\int_0^1\left(\frac{dp}{dx}\right)dx. \quad (24)$$

RESULTS AND DISCUSSION

In this section, we have presented the graphical results of the solutions. The expression for pressure rise is calculated numerically using mathematics software. The pressure rise Δp_λ for different values of couple stress parameter γ and slip parameter β are plotted in Figs. 1 and 2. It is observed from Fig.1, that the pressure rise increases for small values of θ $(0\le\theta\le5.1$ peristaltic pumping) with the increase in γ and for large of θ $\left(5.1\le\theta\le10\right.$ augmented pumping$\left.\right)$ the pressure rise decreases. From Fig. 2, it is observed that with the increase in β, the pressure rise decrease for small values of θ, and at the end the behavior is reverse. The pressure

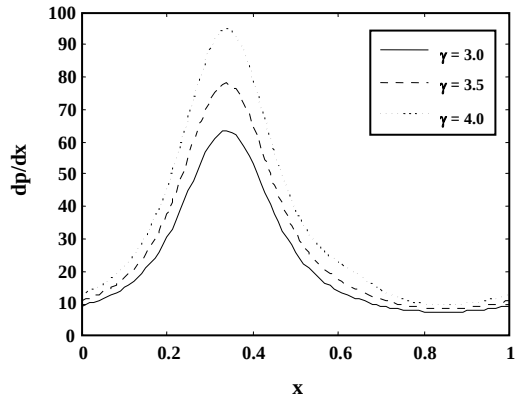

Fig. 3: Variation of Δp_λ with θ for different values of β at a=0.7, b=1.2, d=2, $\varphi = \frac{\pi}{2}$, M=1, E=6, γ=3.5.

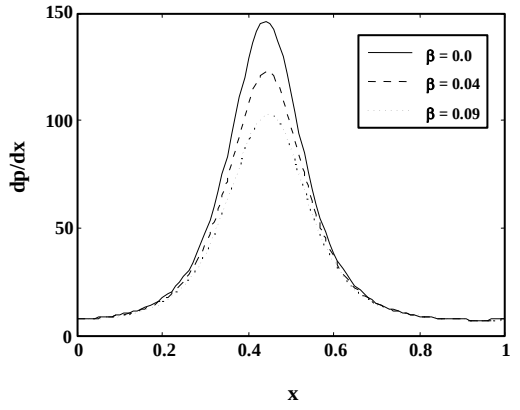

Fig. 4: Variation of (dp/dx) with x for different values of β at a=0.7, b=1.2, d=2, $\phi = \frac{\pi}{6}$, M=1, E=5, θ=-2, γ=3.5.

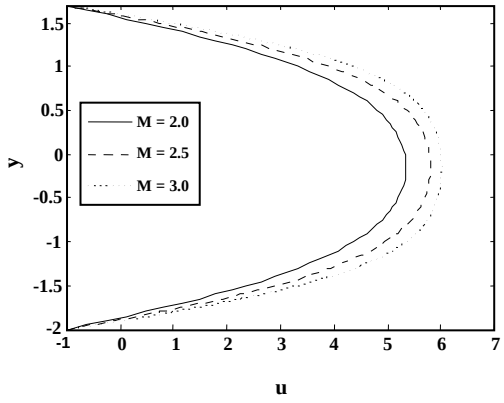

Fig. 5: Velocity profile for different values of M at a=0.5, b=1.2, d=2, γ=2, $\phi = \frac{\pi}{2}$, θ=2, β=0.001, x=0, E=6, dp/dx=2.0.

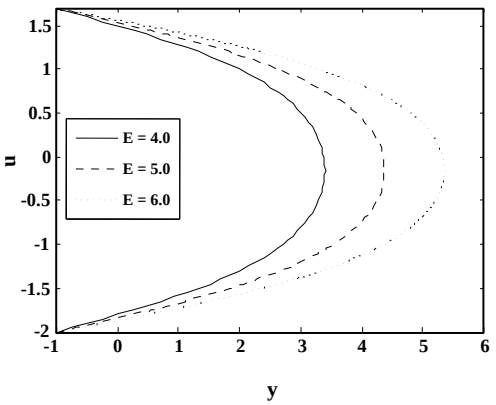

Fig. 6: Velocity profile for different values of E at a=0.7, b=1.2, d=2, γ=2, M=3, θ=2, $\phi = \frac{\pi}{2}$, x=0, β=0.001, dp/dx=2.0.

gradient for different values of γ and β against x is plotted in Figs. 3 and 4. It is depicted from the figures that for $x \in [0, 0.15]$ and $x \in [0.8, 1]$, the pressure gradient is small i.e. the flow can easily pass while in the narrow part of the channel $x \in [0.15, 0.8]$, to retain the same flux large pressure gradient is required. This phenomena is physically valid. Moreover in the narrow part of the channel, the pressure gradient increases with the increase in couple stress parameter γ and decreases with the increase in β (slipparameter). The velocity field for different values of M and E against γ are shown in Figs. 5 and 6. It is concluded from Fig. 5 and Fig. 6 that the velocity profile increases with an increase in M and E. The induced magnetic field h_x against γ for different values of magnetic Reynold number R_m and slip parameter β are plotted in Figs. 7 and 8. It is observed from the figures that with the increase in R_m and slip parameter β, h_x increases in upper half of the channel while in the lower half the behavior is opposite. The magnetic force function Φ for different values of E and R_m are shown in Figs. 9 and Fig. 10. It is observed from the Figs. 9 and 10 that the magnitude value of magnetic force function Φ increases with an increase in E. The current density distribution J_z for different values of M and Q are shown in Fig. 11 and Fi.g 12. It is depicted from the Figs. that the current density distribution J_z decreases with an increase in M and increases with an increase in θ

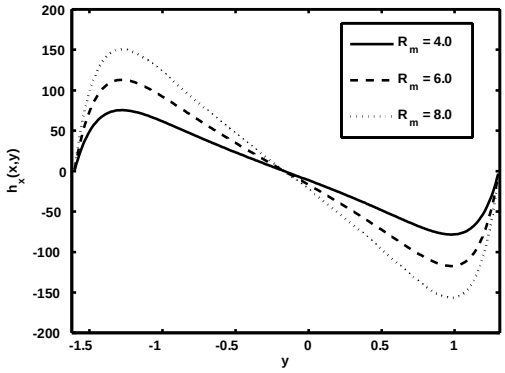

Fig.7: Variation of axial induced magnetic field across the channel for different values of R_m at a=0.7, b=1.2, d=2, $\phi = \pi/2$, d=2, M=3, E=6, β=0.01, γ=6, θ=-3.

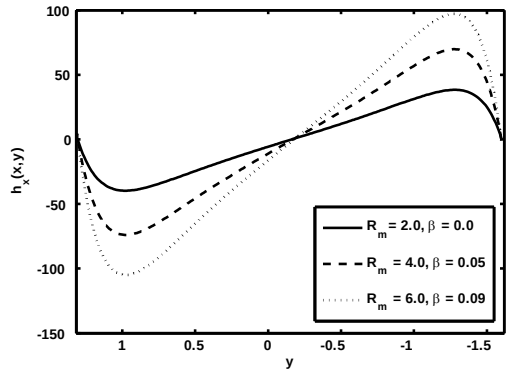

Fig. 8: Variation of axial induced magnetic field across the channel for different values of R_m and β at a=0.7, b=1.2 d=2, $\phi = \pi/2$, E=6, M=3, γ=6, θ=-3.

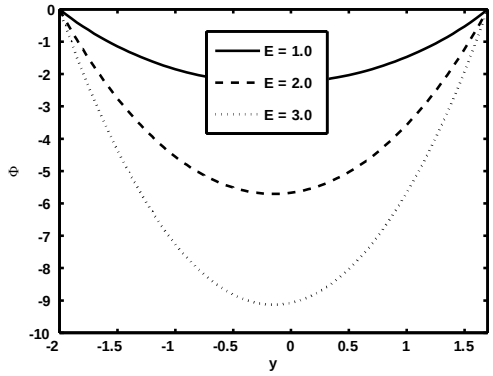

Fig. 9 : Variation of magnetic force function Φ with y for different values of E for fixed a=0.7, b=1.2, d=2, $\phi = \pi/2$, M=4, γ=3, θ=2, x=0, R_m=2, β=0.5.

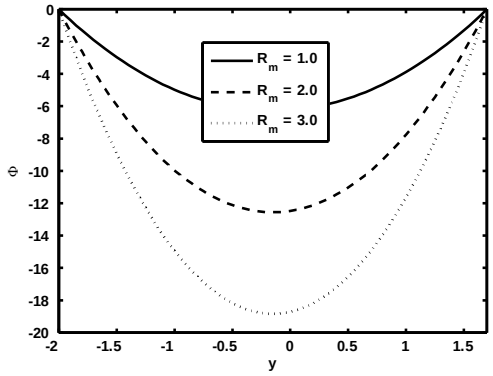

Fig. 10 : Variation of magnetic force function Φ with y for different values of R_m for fixed a=0.7, b=1.2, d=2, $\phi = \pi/2$, M=4, γ=3, θ=2, x=0, E=4, β=0.5.

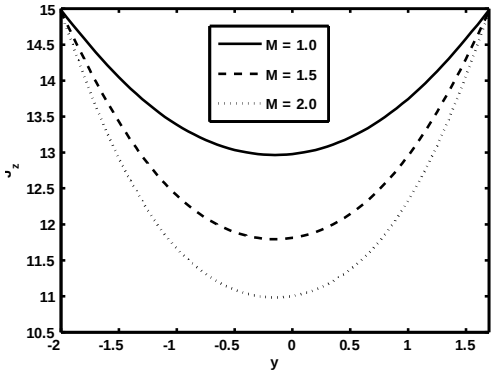

Fig. 11: Variation of current density distribution J_z with y for different values of M for fixed a=0.7, b=1.2, d=2, $\phi = \pi/2$, E=4, γ=3, θ=2, x=0, R_m=3, β=0.01.

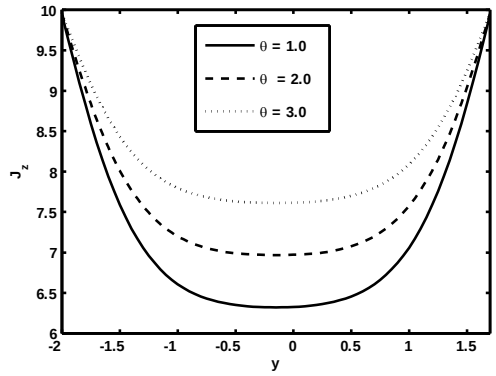

Fig. 12: Variation of current density distribution J_z with y for different values of θ for fixed a=0.7, b=1.2, d=2, $\phi = \pi/2$, E=4, γ=3, M=4, x=0, R_m=2, β=0.01.

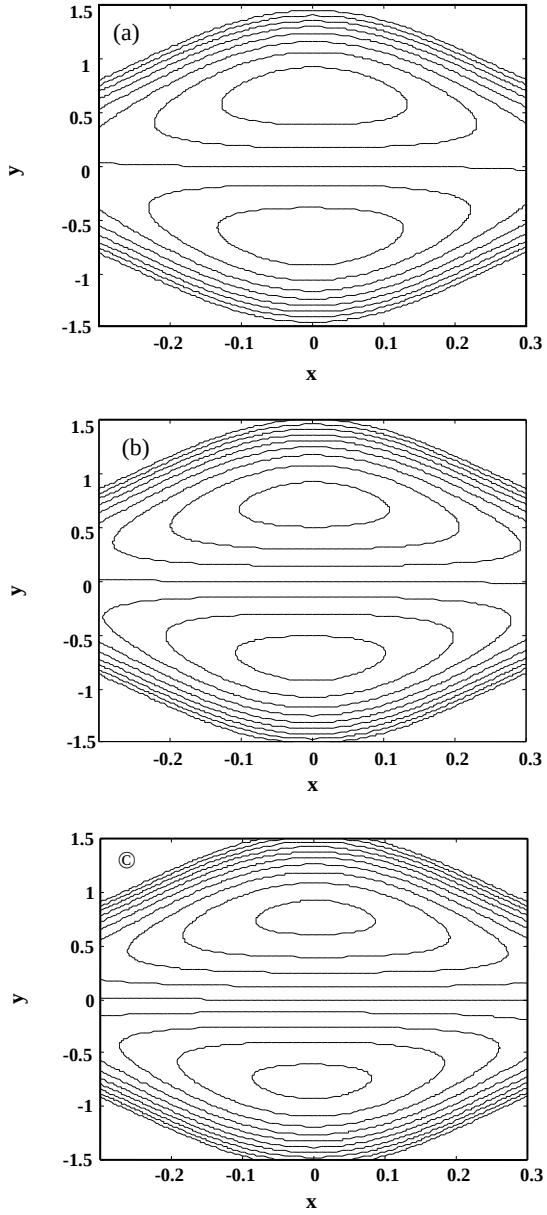

Fig. 13: Stream lines for different values of θ. Fig (a) for θ=1.5. Fig. (b) for θ=1.6. Fig. (c) for θ=1.7. The other parameters are γ=8, b=0.5, d=1, E=4, a=0.5, ϕ=0.02, M=3, β=0.01.

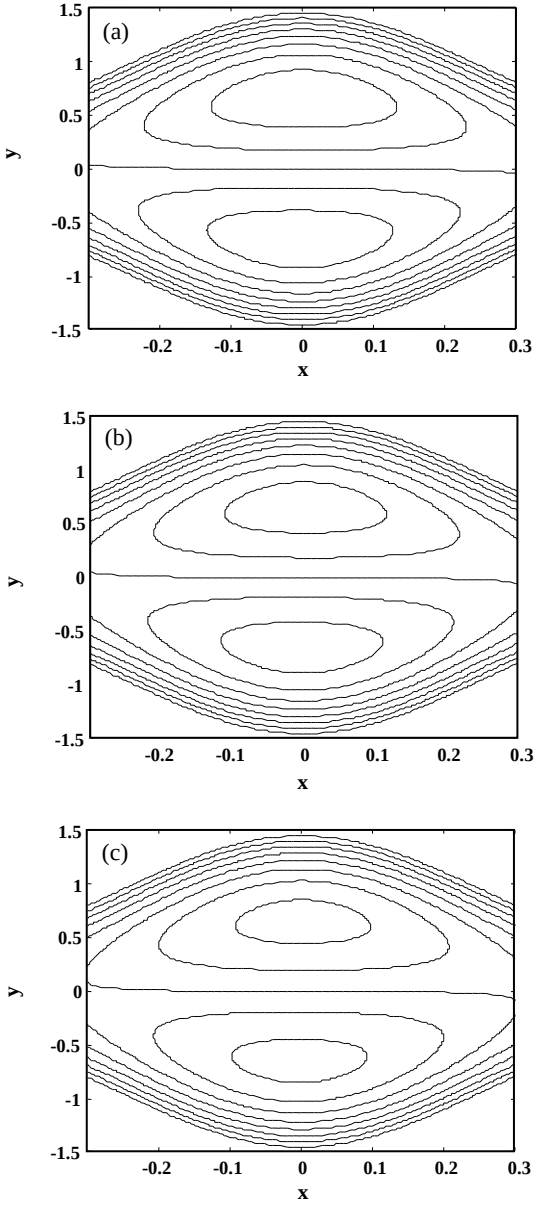

Fig. 14: Stream lines for different values of β Fig. (a) for β=0.01. Fig. (b) for β=0.02. Fig. (c) for β=0.03. The other parameters are b=0.5, d=1, E=4, γ=8, a=0.5, θ=1.5, ϕ=0.02, M=3.

Trapping phenomena

Another interesting phenomena in peristaltic motion is trapping. It is basically the formation of an internally circulating bolus of fluid by closed stream lines. This trapped bolus pushed a head along peristaltic waves. Figs. 13 to 15 illustrate the stream lines for different values of θ, β and γ. The effect of the θ (flowrate) and slip parameter β on the trapping are illustrated in Figs. 13 and 14. It is observed that with the increase in θ and β , the size of the trapping bolus decreases. It is concluded from Fig. 15 that with the increase in couple stress parameter γ the size of the trapped bolus increases.

CONCLUSIONS

In the present paper we have discussed the Influence of Induced magnetic field and partial slip on the

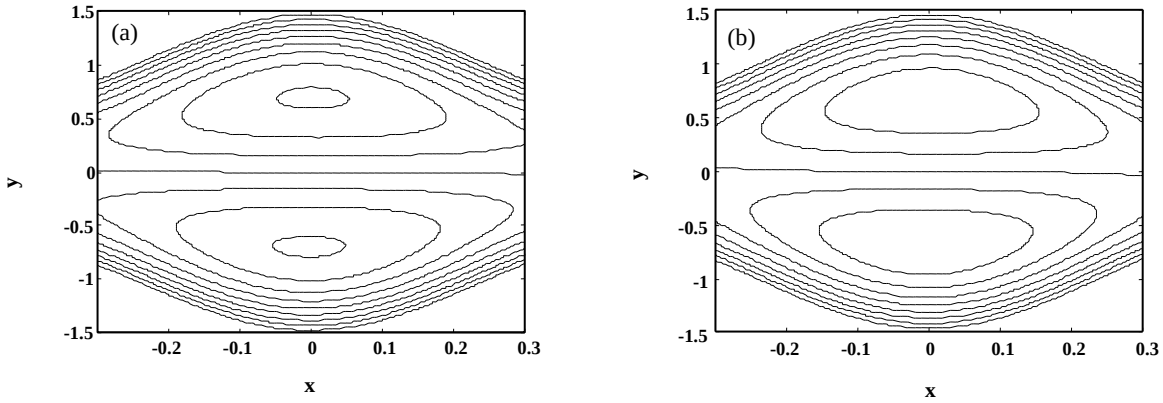

Fig. 15: Stream lines for different values of γ Fig. (a) for γ=5. Fig. (b) for γ=6.5. The other parameters are b=0.5, d=1, a=0.5, E=4, M=2, ϕ=0.02, θ=1.5, β=0.01.

peristaltic flow of a couple stress fluid in an asymmetric channel. The governing two dimensional equations are simplified using long wave length approximation. The exact solution of simplified equations is calculated. The results are discussed through graphs. We conclude the following observations:

1) It is observed that in the peristaltic pumping region the pressure rise increases with the increase in couple stress parameter γ and decreases with the increase in the slip parameter β

2) The pressure gradient increases with the increase in couple stress parameter γ and decreases with the increase in β.

3) The velocity field decreases with the increase in M and slip parameter β

4) The axial induced magnetic field h_x increases in upper half of the channel while in the lower half the behavior is opposite with the increase in R_m and slip parameter β.

5) It is observed that with the increase in θ and β, the size of the trapping bolus decreases and with the increase in couple stress parameter γ the size of the trapped bolus increases.

Received : May 5, 2011 ; Accepted : Apr. 28, 2013

REFERENCES

[1] Stokes V.K., Couple Stress Fluid, *Physics of Fluids*, **9**: 1709-1715 (1966).

[2] Mekheimer Kh. S., Abd Elmaboud Y., Peristaltic Flow of a Couple Stress Fluid in an Annulus; Application of an Endoscope, *Physica A*, **387**:2403-2415 (2008).

[3] Mekheimer Kh. S., Peristaltic Transport of a Couple Stress Fluid in a Uniform and Non-Uniform Channels, *Biorheology*, **39**, 755-765 (2002).

[4] Nabil T. M. EL-Dabe, Salwa M. G. EL-Mohandis, Effects of Couple Stresses on Pulsatile Hydromagnetic Poiseuille, *Fluid Dynamics Research*, **15**: 313-324 (1995).

[5] Stokes V. K., Effects of Couple Stresses in Fluids on the cCreeping Flow Past a Sphere, *Physics of Fluids*, **14**: 1580-1582 (1971).

[6] Valanis K.C., Sun C.T., Poiseuille Flow of a Fluid with Couple Stress with Application to Blood Flow, *Biorheology*, **6**: 85-97 (1969).

[7] EL Shehawey E.F., Mekheimer Kh. S., Couple Stresses in Peristaltic Transport of Fluids, *Journal of Physics D: Applied Physics*, **27**: 1163-1170 (1994).

[8] Mekheimer Kh.S., Effect of Magnetic Field on Peristaltic Flow of a Couple Stress Fluid, *Physics Letters A*, **372**: 4271-4278 (2008).

[9] Ali N., Hayat T., Sajid M., Peristaltic Flow of a Couple Strees Fuid in an Asymmetric Channel, *Biorheology*, **44**: 125-138 (2007).

[10] Mekheimer Kh.S., El Shehawey E. F., Alaw A. M., Peristaltic Motion of a Particle Fluid Suspension in a Planar Channel, *International Journal of Theoretical Physics*, **37**: 2895-2920 (1998).

[11] Mishra M., Rao A.R., Peristaltic Transport of a Newtonian Fluid in an Asymmetric Channel, *Zeitschrift Fur Angewandte Mathematik and Physik*, **54**: 532-550 (2004).

[12] Misery A.E.M., El Shehawey E.F., Hakeem A.A., Peristaltic Motion of an Incompressible Generalized Newtonian Fluid in a Planar Channel, *Journal of Physical Society of Japan*, **65**, 3524-3529 (1996).

[13] Shapiro A.H., Jaffrin M.Y., Weinberg S.L., Peristaltic Pumping with Long Wave Length at Low Reynolds Number, *Journal of Fluid Mechanics*, **37**: 799-825 (1969).

[14] Nadeem S., Akram S., Slip Effects on the Peristaltic Flow of a Jeffrey Fluid in an Asymmetric Channel Under the Effect of Induced Magnetic Field, *International Journal for Numerical Methods in Fluids*, **63**: 374-394 (2010).

[15] Haroun M. H., Effect of Deborah Number and Phase Difference on Peristaltic Transport in an Asymmetric Channel, Communications in Nonlinear *Science and Numerical Simulation*, **12**: 1464-1480 (2007).

[16] Haroun M. H., Non-Linear Peristaltic Flow of a Fourth Grade Fluid in an Inclined Asymmetric Channel, *Computer and Material Sciences*, **39**: 324-333 (2007).

[17] Kotkandapani M., Srinivas S., Non-Linear Peristaltic Transport of Newtonian Fluid in an Inclined Asymmetric Channel Through a Porous Medium, *Physics Letters A*, **372**: 1265-1276 (2008).

[18] Mekheimer Kh.S., Abd elmaboud Y., The Influence of Heat Transfer and Magnetic Field on Peristaltic Transport of a Newtonian Fluid in a Vertical Annulus: An Application of an Endoscope, *Physics Letters A*, **372**: 1657-1665 (2008).

[19] Wang Y., Hayat T., Hutter K., On Non-Linear Magnetohydrodynamics Problems of an Oldroyd-6-Constant Fluid, *International Journal of Non-Linear Mechanics*, **40**: 40-58 (2005).

[20] Akram S., Nadeem S., Influence of Induced Magnetic Field and Heat Transfer on the Peristaltic Motion of a Jeffrey Fluid in an Asymmetric Channel: Closed form Solutions, *Journal of Magnetism and Magnetic Materials*, **328**: 11-20 (2013).

[21] Akram S., Nadeem S., Hanif M., Numerical and Analytical Treatment on Peristaltic Flow of Williamson Fluid in the Occurrence of Induced Magnetic Field, *Journal of Magnetism and Magnetic Materials*, **346**: 142-151 (2013).

[22] Nadeem S., Akram S., Akbar N.Sh., Simulation of Heat and Chemical Reactions on Peristaltic Flow of a Williamson Fluid in an Inclined Asymmetric Channel, *Iranian Journal of Chemistry and Chemical Engineering (IJCCE)*, **32**: 93-107 (2013).

[23] Mekheimer Kh.S., Effect of the Induced Magnetic Field on Peristaltic Flow of a Couple Stress Fluid, *Physics Letters A*, **372**: 4271-4278 (2008).

[24] Srivastava L.M., Agrawal R.P., Oscillating Flow of a Conducting Fluid with Suspension of Spherical Particles, *Journal of Applied Mechanics*, **47**: 196-199 (1980).

[25] S. Nadeem, Safia Akram, Peristaltic Transport of a Hyperbolic Tangent Fluid Model in an Asymmetric Channel, *Z. Naturforsch*, **64a**: 559-567 (2009).

[26] Nadeem S., Akram S., Peristaltic Flow of a Williamson Fluid in an Asymmetric Channel, *Communications in Nonlinear Science and Numerical. Simulation*, **15**: 1705-1716 (2010).

[27] Fu-Yun Zhao, Di Liu, Guang-Fa Tang, Natural Convection in a Porous Enclosure with a Partial Heating and Salting Element, *International Journal of Thermal Sciences*, **47**: 569-583 (2008).

[28] Donald Ariel P., Axisymmetric Flow Due to a Stretching Sheet with Partial Slip, *Computers & Mathematics with Applications*, **54**: 1169-1183 (2007).